Itinerant-electron metamagnetism of MnSi at high pressure

H. Yamada* and K. Terao
Department of Physics, Faculty of Science, Shinshu University, Matsumoto 390-8621, Japan
(Received 16 March 1998)

Metamagnetic behaviors observed recently for MnSi at high pressure are discussed by using the electronic structures calculated in a self-consistent linear muffin-tin orbital method within the atomic-sphere approximation. It is shown that the ferromagnetic state with the moment larger than about $0.4\mu_B$/Mn is stable at large lattice constants, while the paramagnetic state becomes stable at smaller lattice constants. By the fixed-spin-moment method the difference $\Delta E(M)$ between the total energies of the ferromagnetic and paramagnetic states is calculated as a function of magnetic moment M near the critical lattice constant. The calculated $\Delta E(M)$ is fitted to a form of the power series of M^2 up to the term of M^{10}. Pressure dependences of the magnetization and susceptibility observed for MnSi are compared with the calculated results. Temperature dependences of the metamagnetic transition and susceptibility are also discussed by taking into account the effects of spin fluctuations and by using the expansion coefficients in the calculated $\Delta E(M)$. Metamagnetic behaviors observed for MnSi at high pressure are shown to be described very well by the present model. [S0163-1829(99)02510-2]

I. INTRODUCTION

The cubic B20-type intermetallic compound MnSi is known as a helimagnet with a long-wavelength (180 Å) spin structure.[1] The helical spin state was observed to change into an induced ferromagnetic one by external magnetic fields. The induced ferromagnetic moment is about $0.4\mu_B$/Mn at 6.2 kOe and increases rather strongly with increasing field even at 150 kOe.[2] These experimental facts, together with the neutron-scattering measurements[3] and nuclear spin-lattice relaxation time measurements,[4] show that this compound is a typical weak itinerant-electron magnet. On the other hand, these magnetic properties have been discussed theoretically on the self-consistent renormalization theory for spin fluctuations.[5] Calculations of the electronic structure have also been carried out.[6,7] The density-of-states (DOS) at the Fermi level was shown to be high and the observed de Haas–van Alphen frequencies were found to be well described by the calculated band structures.

Recent experimental results, however, show that MnSi is not a simple itinerant-electron magnet at high pressure. The magnetic phase transition at the critical temperature T_C is of the second-order at ambient pressure. With increasing pressure it changes to the first-order transition and, subsequently, T_C collapses to zero at higher pressure than 14.6 kbar.[8] The paramagnetic susceptibility shows a maximum at about 10 K in its temperature dependence at higher pressure.[8,9] The measurements of the induced moment by the magnetic field were also performed at higher pressures and a metamagnetic transition from the nonmagnetic to ferromagnetic state has been observed at low temperature.[9] These phenomena of the susceptibility maximum and metamagnetic transition are characteristics of the itinerant-electron metamagnetism (IEMM).[10,11] They have also been observed for the cubic Laves phase compounds YCo_2 and $LuCo_2$, pyrite compound $Co(S,Se)_2$ and others at ambient pressure.[12,13] Recently, the metamagnetic transition has been observed for CoS_2 under the high pressure.[14,15]

The spin-fluctuation model for IEMM was proposed on the Landau-Ginzburg free energy expanded up to the six power of magnetization M.[16] When the magnetic energy $\Delta E(M)$ is written as

$$\Delta E(M)=\frac{1}{2}aM^2+\frac{1}{4}bM^4+\frac{1}{6}cM^6, \tag{1.1}$$

with $a>0$, $b<0$, and $c>0$, the ferromagnetic state was shown to be stable for $ac/b^2<3/16$. For $5/28<ac/b^2<3/16$ the magnetic transition at T_C is of the first-order, while it is of the second-order for $ac/b^2<5/28$.[17] For $3/16<ac/b^2<9/20$ the metamagnetic transition takes place at low temperature.[11] The paramagnetic susceptibility shows a maximum for $ac/b^2>5/28$.[16] These anomalous properties are very similar to the observed ones of MnSi at high pressure.[8,9] The aim of the present paper is to study the magnetic properties of MnSi on the spin-fluctuation model with the calculated electronic structures.

Calculated results of the electronic structure and local moments of MnSi are given as a function of the lattice constant in Sec. II. By a fixed-spin-moment method the difference $\Delta E(M)$ for given values of M is calculated in Sec. III. The obtained result of $\Delta E(M)$ is found to be fitted to a form of the power series of M^2 up to the term of M^{10}. In Sec. IV, the spin-fluctuation model for IEMM (Ref. 16) is extended to the present case of $\Delta E(M)$. Calculated results are compared with observed ones in Sec. V. Our conclusion and discussion are given in Sec. VI.

II. ELECTRONIC STRUCTURE

The electronic structure of MnSi is calculated by a self-consistent linear muffin-tin orbital method and the atomic-sphere approximation (ASA) with the exchange-correlation potential by von Barth and Hedin.[18] MnSi with the B20-type structure contains four Mn and four Si atoms at (u,u,u), $(\frac{1}{2}+u,\frac{1}{2}-u,-u)$, $(-u,\frac{1}{2}+u,\frac{1}{2}-u)$, $(\frac{1}{2}-u,-u,\frac{1}{2}+u)$ in a cubic unit cell, where $u_{Mn}=0.137$ and $u_{Si}=0.845$.[6] Radii of atomic spheres for Mn and Si used in the

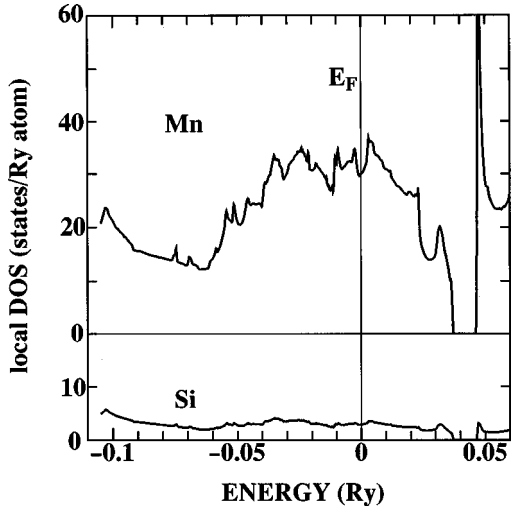

FIG. 1. Calculated local DOS in the paramagnetic state at the observed lattice constant. E_F denotes the Fermi level.

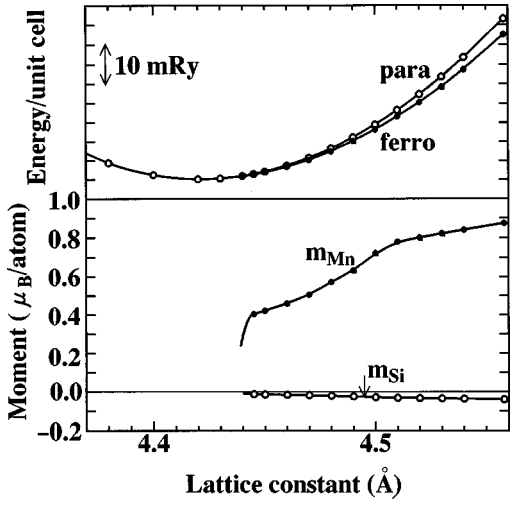

FIG. 2. Total energies in the paramagnetic and ferromagnetic states (upper panel) and local magnetic moments (lower panel) calculated as a function of the lattice constant.

ASA are taken to be the same as each other, as the total energy was confirmed to become almost minimum for them. In the present calculation the spin-orbit interaction was not included, although the calculations are scalar relativistic, including mass velocity and Darwin terms. Self-consistent calculations are carried out at 176 **k** points in the irreducible 1/24 Brillouin zone. The convergence in charge density was achieved so that the root-mean square of moments of the occupied partial density of states becomes smaller than 10^{-6}. The basic sets of functions with angular momenta up to $l=3$ on Mn and Si atoms were adopted.

Figure 1 shows the calculated result of the local DOS curves for Mn and Si at the observed lattice constant 4.558 Å in the nonmagnetic state. The shape of DOS and the position of the Fermi level E_F are very similar to those calculated previously.[6,8] Main characters of DOS near E_F are of the d states of Mn atom. It can be seen that E_F lies at a tiny minimum on the broad peak of the local DOS, which has been shown also in Ref. 8.

By the spin-polarized band calculation the total energy and local moments are obtained as a function of lattice constant. The upper panel of Fig. 2 shows the total energies in the ferromagnetic and paramagnetic states. The calculated minimum energy appears in the paramagnetic state at 4.42 Å, which is about 3% smaller than the observed one. The total energy in the helimagnetic state is not estimated in this paper. However, it will be close to that in the ferromagnetic state as the wavelength of the helical spin ordering is very long. The disagreement between the calculated and observed lattice constant comes probably from the use of the ASA in the present calculation. Anyhow, the difference between the total energies in the ferromagnetic and paramagnetic states is very small as shown in the upper panel of Fig. 2. The local moments on Mn and Si atoms are shown in the lower panel of Fig. 2. A small and negative moment is induced on Si atoms. This is due to the hybridization between $3d$ states of Mn and $3p$ states of Si. The Mn moment disappears abruptly from about $0.4\mu_B$/atom at about 4.44 Å.

III. ESTIMATION OF $\Delta E(M)$

Numerical calculations of magnetic energy $\Delta E(M)$ for MnSi are carried out at several lattice constants by the fixed-spin-moment method.[19] By this method the total energy is obtained for given moment M, i.e., by fixing the numbers of electrons with up and down spins. In this case, the Fermi levels in the up and down spin bands are not equal to each other because the equilibrium condition is not satisfied for arbitrary M. At the equilibrium M two Fermi levels coincide with each other. The total magnetic energy becomes minimum or maximum at this value of M.

The calculated results of $\Delta E(M)$ in the fixed-spin-moment method are shown in Fig. 3. The numbers shown in the figure denote the lattice constants. It can be clearly seen that the curve of $\Delta E(M)$ is rather flat near $M=0$ and is not expressed in a simple form such as $\frac{1}{2}aM^2+\frac{1}{4}bM^4$ near the critical lattice constant, where the ferromagnetic moment disappears abruptly. In fact, $\Delta E(M)$ has two minima at $M=0$ and finite M near 4.44 Å. The calculated values of $\Delta E(M)$ are fitted very well to a form as

$$\Delta E(M)=\frac{1}{2}aM^2+\frac{1}{4}bM^4+\frac{1}{6}cM^6+\frac{1}{8}dM^8+\frac{1}{10}eM^{10}, \tag{3.1}$$

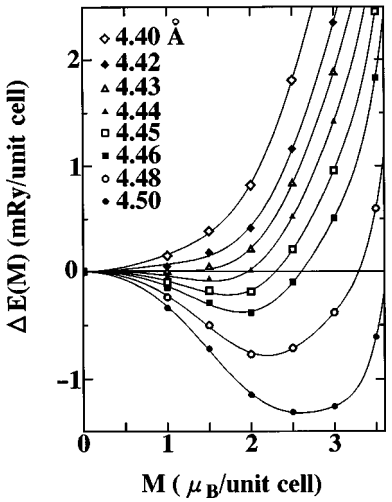

FIG. 3. Calculated results of $\Delta E(M)$ as a function of magnetic moment M. Numbers shown in the figure denote the lattice constants in Å.

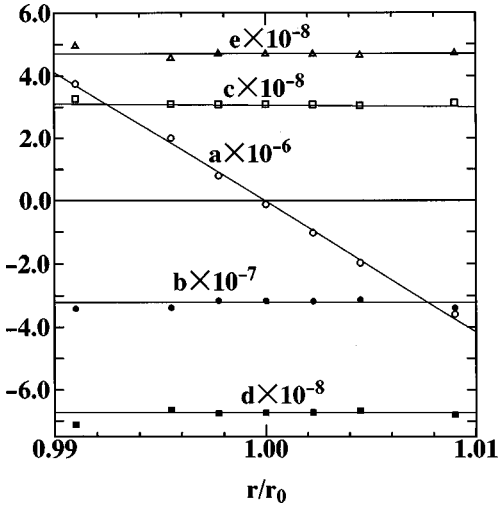

FIG. 4. Estimated values of a in Oe/(μ_B/f.u.), b in Oe/(μ_B/f.u.)^3, c in Oe/(μ_B/f.u.)^5, d in Oe/(μ_B/f.u.)^7, and e in Oe/(μ_B/f.u.)^9, as a function of r/r_C.

which is shown by thin curves in Fig. 3.

The estimated values of the coefficients a, b, c, d, and e in Eq. (3.1) are shown in Fig. 4 as a function of r/r_C by open circles, closed circles, open squares, closed squares, and open triangles, respectively. Here, r is the lattice constant and $r_C = 4.44$ Å where the coefficient a in Eq. (3.1) becomes zero. It should be mentioned that a decreases linearly with increasing r. Other coefficients b, c, d, and e do not depend so much on r. They are evaluated as

$$a(r) = 4.131\times 10^8(1-r/r_C),$$

$$b = -3.209\times 10^7,$$

$$c = 3.107\times 10^8, \tag{3.2}$$

$$d = -6.777\times 10^8,$$

$$e = 4.698\times 10^8,$$

in the units of Oe/(μ_B/f.u.), Oe/(μ_B/f.u.)^3, Oe/(μ_B/f.u.)^5, Oe/(μ_B/f.u.)^7, and Oe/(μ_B/f.u.)^9, respectively, as shown by thin lines in Fig. 4.

IV. SPIN-FLUCTUATION MODEL

In this section the spin-fluctuation model for IEMM (Ref. 16) is extended to the case of $\Delta E(M)$ given by Eq. (3.1). The magnetic free energy is written as

$$\Delta F = \frac{1}{V}\int d^3r \Delta f(\mathbf{r}), \tag{4.1}$$

where free-energy density $\Delta f(\mathbf{r})$ is a sum of the local and nonlocal ones, $\Delta f_l(\mathrm{r})$ and $\Delta f_{nl}(\mathrm{r})$, as

$$\Delta f(\mathbf{r}) = \Delta f_l(\mathbf{r}) + \Delta f_{nl}(\mathbf{r}), \tag{4.2}$$

$$\Delta f_l(\mathbf{r}) = \frac{1}{2}a|\mathbf{m}(\mathbf{r})|^2 + \frac{1}{4}b|\mathbf{m}(\mathbf{r})|^4 + \frac{1}{6}c|\mathbf{m}(\mathbf{r})|^6 + \frac{1}{8}d|\mathbf{m}(\mathbf{r})|^8 + \frac{1}{10}e|\mathbf{m}(\mathbf{r})|^{10}, \tag{4.3}$$

$$\Delta f_{nl}(\mathbf{r}) = \frac{1}{2}J|\nabla\cdot\mathbf{m}(\mathbf{r})|^2. \tag{4.4}$$

Here J is the exchange stiffness constant written by the notation D in Ref. 16. $\mathbf{m}(\mathbf{r})$ and V are the magnetization density and the volume of crystal. The coefficients a, b, c, d, and e in Eq. (4.3) are those obtained in the previous section.

In Eq. (4.4) we neglect the higher-order derivatives of $\mathbf{m}(\mathbf{r})$. As pointed out by Edwards,[20] in MnSi the enhancement of the Curie constant and the forward-scattering peak in neutron data[21] above T_N are attributed to the long-wavelength spin fluctuations. Then, it can be inferred that only the lowest gradient term in the nonlocal free-energy density will be enough to discuss the MnSi problem. It should be noted here that the value of J in Eq. (4.4) can be calculated in the local spin-density approximation.[22] However, in the present paper, we did not estimate it and the calculation of J for MnSi is left for future work.

The equation of state for the magnetic field H and bulk magnetization M is given by

$$H = \left\langle \frac{\partial \Delta F}{\partial M} \right\rangle = A(T)M + B(T)M^3 + C(T)M^5 + D(T)M^7 + E(T)M^9, \tag{4.5}$$

where $\langle\ \rangle$ denotes a thermal average and

$$A(T) = \chi(T)^{-1} = a + \frac{5}{3}b\xi(T)^2 + \frac{35}{9}c\xi(T)^4 + \frac{35}{3}d\xi(T)^6 + \frac{385}{9}e\xi(T)^8, \tag{4.6}$$

$$B(T) = b + \frac{14}{3}c\xi(T)^2 + 21d\xi(T)^4 + \frac{308}{3}e\xi(T)^6, \tag{4.7}$$

$$C(T) = c + 9d\xi(T)^2 + 66e\xi(T)^4, \tag{4.8}$$

$$D(T) = d + \frac{44}{3}e\xi(T)^2, \tag{4.9}$$

$$E(T) = e. \tag{4.10}$$

Here, $\xi(T)^2$ in Eqs. (4.6)–(4.9) is the mean-square amplitude of spin fluctuations defined as

$$\xi(T)^2 = \xi_\parallel(T)^2 + 2\xi_\perp(T)^2, \tag{4.11}$$

where

$$\xi_\parallel(T)^2 = \frac{1}{V}\sum_{q(\neq 0)} \langle|m_\parallel(\mathbf{q})|^2\rangle, \tag{4.12}$$

$$\xi_\perp(T)^2 = \frac{1}{V}\sum_{q(\neq 0)} \langle|m_\perp(\mathbf{q})|^2\rangle, \tag{4.13}$$

and $m_{\parallel}(\mathbf{q})$ and $m_{\perp}(\mathbf{q})$ are Fourier components of the fluctuating magnetization densities parallel and perpendicular to H, respectively. The coefficient $A(T)$ in Eq. (4.5) is the inverse of susceptibility, $\chi(T)^{-1}$.

The derivation of Eq. (4.5) is essentially done in the same way as in Ref. 16. Shimizu[23] has also discussed spin fluctuations by using the energy expanded up to the term of M^8. In the present paper, we assumed that $\xi_{\parallel}(T)^2=\xi_{\perp}(T)^2$. An explicit expression for $\xi(T)^2$ is not given here. It is written in terms of the dynamical spin susceptibility and known to increase with increasing T as T^2 at low T and as T at high T.[24,25] That is, $\xi(T)^2$ is a monotonically increasing function of T. The zero-point spin fluctuations are not considered here.

The values of $A(T)$, $B(T)$, $C(T)$, $D(T)$, and $E(T)$ for MnSi were thus evaluated as a function of $\xi(T)^2$ or T. It is mentioned here that the following relations between $A(T)$, $B(T)$, $C(T)$, $D(T)$, and $E(T)$ are obtained from Eqs. (4.6)–(4.10) as

$$B(T)=\frac{3}{5}\partial A(T)/\partial\xi(T)^2, \tag{4.14}$$

$$C(T)=\frac{3}{14}\partial B(T)/\partial\xi(T)^2, \tag{4.15}$$

$$D(T)=\frac{1}{9}\partial C(T)/\partial\xi(T)^2, \tag{4.16}$$

$$E(T)=\frac{3}{44}\partial D(T)/\partial\xi(T)^2. \tag{4.17}$$

That is, $B(T)$, $C(T)$, $D(T)$, and $E(T)$ are obtained by the derivatives of $A(T)$ with respect to $\xi(T)^2$.

V. COMPARISON WITH EXPERIMENT

A. Pressure dependences of susceptibility and magnetization at low temperature

The dependence of a on the lattice constant r shown in Fig. 4 can be compared with the observed pressure dependence of susceptibility[8] at high pressures. The lattice constant at zero pressure r_0 is estimated so that the value of a at r_0 coincides with the extrapolated one, -1021 cm^3/emu, from the observed susceptibilities[8] at high pressure. We get $r_0=4.444$ Å, being about 2.5% smaller than the observed one. The value of r_0 is very close to r_C defined in Eq. (3.2). By using the observed compressibility[26] the value of $\partial a/\partial P$ is obtained as 260 cm^3/emu kbar, which is about twice that of the observed one.[8] As the value of $\partial a/\partial P$ is very sensitive to the value of r_0, the agreement between the calculated and observed results is not unsatisfactory.

MnSi is a helimagnet without magnetic field. However, under a weak magnetic field 6.2 kOe, it becomes ferromagnetic.[2] Then, our results obtained above can be compared with the observed ones under the magnetic field. From Fig. 2 the magnetic moment of Mn is found to be about $0.4\mu_B$/atom at the lattice constant r_0, which is rather close to the observed one[2] under the magnetic field. The P dependence of the magnetic moment M can be also estimated from Fig. 2 near r_0. By using the observed compressibility[26] we get $d\ln M/dP=-0.93\times10^{-2}$ kbar^{-1}, which is close to the observed ones[2,27] -1.15×10^{-2} kbar^{-1} and -1.27×10^{-2} kbar^{-1}.

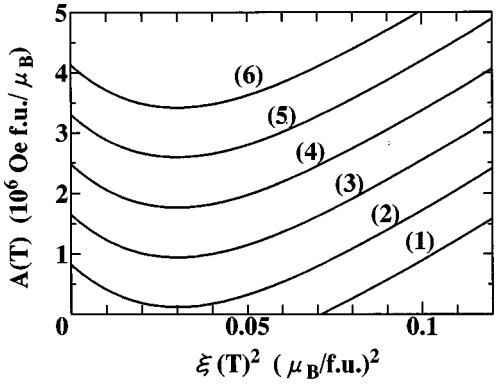

FIG. 5. Calculated value of $A(T)$ as a function of $\xi(T)^2$, (1)–(6) for $\delta r/r_C=0.0$, 2.0×10^{-3}, 4.0×10^{-3}, 6.0×10^{-3}, 8.0×10^{-3}, and 1.0×10^{-2}, respectively.

B. Susceptibility maximum

The temperature dependence of $A(T)$ for MnSi is estimated from Eq. (4.6) with the coefficients a, b, c, d, and e given by Eq. (3.2). Calculated results of $A(T)$ are shown in Fig. 5 for several values of $\delta r/r_C$, where $\delta r=r_C-r$. $A(T)$ shows a minimum at $\xi(T_{max})^2\sim0.03$ $(\mu_B/\text{f.u.})^2$, that is, $\chi(T)$ shows a maximum at T_{max}. It is easily shown in the present approximation that the value of $\xi(T_{max})^2$ does not depend on r or P. The minimum of $A(T)$ is a solution of the equation $\partial A(T)/\partial\xi(T)^2=0$, that is, $B(T)=0$ as shown by Eq. (4.14). The solution, $\xi(T_{max})^2$, of this equation is then written only by b, c, d, and e which do not depend on r, or P, as $B(T)$ is given by Eq. (4.7). In this way, we can see that $\xi(T_{max})^2$ does not depend on r or P. The present result is consistent with the observed one[8] where the dependence of T_{max} on P is not significant at the pressure between 7.2 and 16.3 kbar.

Above T_{max}, $A(T)$ increases almost linearly with $\xi(T)^2$, as shown in Fig. 5. The linearity comes from the higher order terms of $\xi(T)^6$ and $\xi(T)^8$ in Eq. (4.6). This result is also consistent with the observed result of the Curie-Weiss behavior of the susceptibility at high T, where $\xi(T)^2$ is proportional to T. However, the present theory breaks down at much higher T. This is because our theory is based on the power expansion of the free-energy density Eq. (4.3) with respect to $|\mathbf{m}(\mathbf{r})|^2$, i.e., $\xi(T)^2$.

In Fig. 6, the estimated values of $A(T)$, $B(T)$, $C(T)$, $D(T)$, and $E(T)$ for $\delta r/r_C=2.0\times10^{-3}$ are shown as a function of $\xi(T)^2$. It can be seen that $A(T)$ shows a minimum at $\xi(T_{max})^2$, where $B(T)$ changes its sign from negative to positive. This is just obtained from Eq. (4.14). Other relations between them, Eqs. (4.15)–(4.17), are also seen in this figure. As $A(T)$ increases linearly with increasing $\xi(T)^2$ at high T, then $B(T)$ tends to a constant and $C(T)$ and $D(T)$ tend to zero at high T. At much higher T, where $\xi(T)^2$ is larger than about 0.1 $(\mu_B/\text{f.u.})^2$, the present theory breaks down as mentioned above.

C. Metamagnetic transition

When a metamagnetic transition from the paramagnetic to ferromagnetic states occurs, the magnetization curve $M(H)$

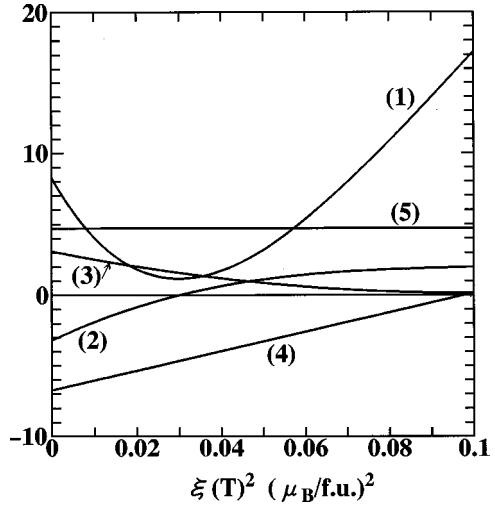

FIG. 6. Calculated values of (1) $A(T)\times 10^5$ in Oe/(μ_B/f.u.), (2) $B(T)\times 10^7$ in Oe/(μ_B/f.u.)^3, (3) $C(T)\times 10^8$ in Oe/(μ_B/f.u.)^5, (4) $D(T)\times 10^8$ in Oe/(μ_B/f.u.)^7, and (5) $E(T)$ in Oe/(μ_B/f.u.)^9, as a function of $\xi(T)^2$ for $\delta r/r_C = 2.0\times 10^{-3}$.

becomes an *S*-like one. Figure 7 shows $M(H)$ curves at 0 K calculated with Eq. (3.2) for several values of $\delta r/r_C$. The critical field H_C is estimated by the Maxwell relation

$$\int_{M_1}^{M_2} dM H(M) - (M_2 - M_1) H_C = 0, \tag{5.1}$$

where

$$H(M) = aM + bM^3 + cM^5 + dM^7 + eM^9, \tag{5.2}$$

and M_1 and M_2 are stable or metastable solution of the equation $H(M)=H_C$.[11] In the present case, the equation $H(M)=H_C$ has three solutions; stable and metastable solutions and one unstable solution. The dotted curves are those in the metastable or unstable state. It is found that the metamagnetic transition at 0 K occurs at a narrow range $2\times 10^{-3} < \delta r/r_C < 4\times 10^{-3}$. For $\delta r/r_C > 4\times 10^{-3}$ no metamagnetic transition occurs. It can be seen in Fig. 7 that the maximum value of H_C is 16 T at $\delta r/r_C = 4\times 10^{-3}$, which is rather smaller than H_C for YCo_2 and $LuCo_2$.[12]

Figure 8 shows the calculated $M(H)$ at finite T for $\delta r/r_C = 2.5\times 10^{-3}$. The critical field H_C is estimated by the

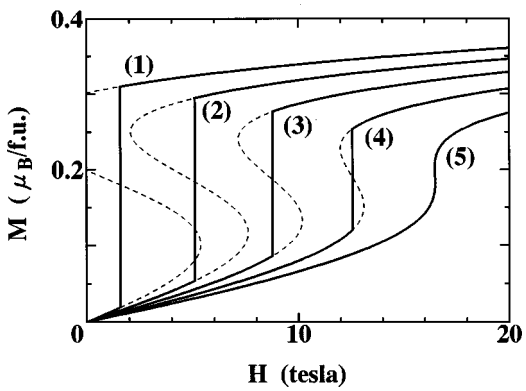

FIG. 7. Calculated results of the magnetization curve at $T=0$, (1)–(5) for $\delta r/r_C = 2.0\times 10^{-3}$, 2.5×10^{-3}, 3.0×10^{-3}, 3.5×10^{-3}, and 4.0×10^{-3}, respectively. The dotted curves are those in the metastable or unstable state.

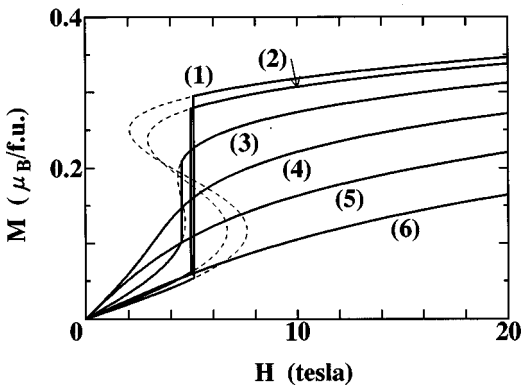

FIG. 8. Calculated results of the magnetization curve, (1)–(6) at $\delta r/r_C = 2.5\times 10^{-3}$ for $\xi(T)=0$, 0.05, 0.10, 0.15, 0.20, and $0.25\mu_B$/f.u., respectively. The dotted curves are those in the metastable or unstable state.

Maxwell relation Eq. (5.1) with $H(M)$ given by Eq. (4.5) and M_1 and M_2 are stable or metastable solutions of the equation $H(M)=H_C$. The dotted curves are those in the metastable state. It is seen in Fig. 8 that the metamagnetic transition disappears at $\xi(T)\sim 0.1$ μ_B/f.u., which is rather smaller than $\xi(T_{max})(=0.17$ μ_B/f.u.). The metamagnetic transition, associated with the hysteresis of magnetization, for MnSi at high pressure is actually observed at lower temperature than T_{max}. For instance, the value of H_C at 15.5 kbar is about 5 kOe below 6.2 K,[9] while T_{max} is 12.4 K.

D. First- and second-order transitions at T_C

In the ferromagnetic region, the magnetic moment M is estimated as a function of $\xi(T)$ without magnetic field H. Figure 9 shows the calculated results of M for $1.76\times 10^{-3} > \delta r/r_C > 1.72\times 10^{-3}$, by using Eq. (3.2) and Eqs. (4.5)–(4.10). The dotted curves in Fig. 9 denote the metastable states. It is found that the second-order transitions at T_C are obtained for $\delta r/r_C < 1.72\times 10^{-3}$. At the narrow range of $1.76\times 10^{-3} > \delta r/r_C > 1.73\times 10^{-3}$ the first-order transition at T_C is obtained. At $\delta r/r_C > 1.77\times 10^{-3}$ the ferromagnetic state becomes unstable without magnetic field.

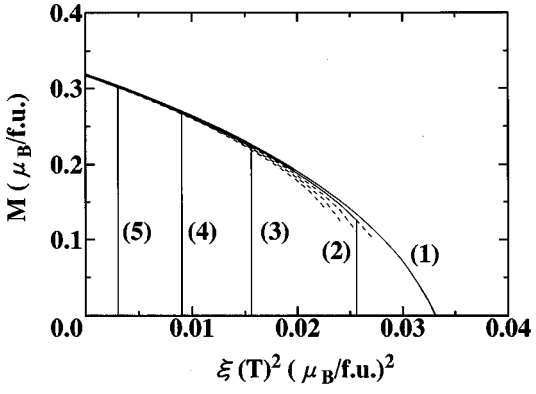

FIG. 9. Calculated results of the magnetization as a function of $\xi(T)^2$, (1)–(5) for $\delta r/r_C = 1.72\times 10^{-3}$, 1.73×10^{-3}, 1.74×10^{-3}, 1.75×10^{-3}, and 1.76×10^{-3}, respectively. The dotted curves are those in the metastable state.

The critical pressure p_C between the ferromagnetic and paramagnetic states can be estimated from the critical lattice constant obtained above and the observed compressibility.[26] The obtained value of p_C is 11.3 kbar, which is a little smaller than the observed one[8,9] 14.6 ± 0.1 kbar. On the other hand, the critical pressure p_1 between the first- and second-order transition at T_C is estimated as 11.0 kbar. The first-order transition at T_C is actually observed only at a narrow range of the pressure between 12 and 14.6 kbar.[8,9] Our estimated values of p_C and p_1 are a little smaller than the observed values. However, they are very sensitive to the value of r_0 estimated in Sec. V A.

VI. CONCLUSION AND DISCUSSION

In the present paper, the fixed-spin-moment calculations for MnSi have been carried out for various lattice constants. The difference $\Delta E(M)$ between the total energies in the nonmagnetic and magnetic states has been found to be fitted to the form of the power expansion of M^2 up to the term of M^{10}. The coefficient a of M^2 in $\Delta E(M)$ was found to depend strongly on the lattice constant, while other coefficients b, c, d, and e were found not to depend so much on the lattice constant.

To discuss the finite-temperature properties, the spin fluctuation model proposed previously[16] has been extended to the present case of $\Delta E(M)$ expanded up to M^{10}. It has been found that the Landau coefficients $B(T)$, $C(T)$, $D(T)$, $E(T)$ in Eq. (4.5) can be written by the derivatives of $A(T)$ with respect to $\xi(T)^2$. This fact could be confirmed by the Arrott plots for the observed $M(H)^2$ and $H/M(H)$ at high pressure.

In the present paper, the effect of zero-point spin fluctuations is neglected. Takahashi and Sakai[28] have emphasized that the zero-point spin fluctuations play an important role in the ground-state properties of IEMM. However, the observed ground-state properties for MnSi at high pressure and low temperature can be well explained by our calculated results based on the band calculations. For instance, a good agreement between the calculated and observed pressure dependences of magnetization was obtained as shown in Sec. V A.

It has been clearly shown in Sec. V B that the calculated value of T_{max}, where the susceptibility reaches a maximum, does not depend on the pressure. The metamagnetic transition was shown in Sec. V C to occur at a narrow range of the lattice constant near the critical one between ferromagnetic and paramagnetic states. The first-order transition at T_C was also shown in Sec. V D to occur at a narrow range of the pressure just below the critical pressure between the ferromagnetic and paramagnetic states. These results are consistent with the observed ones. It can be concluded that the anomalous magnetic properties observed for MnSi at high pressure can be described very well by the present model of the itinerant-electron metamagnetism.

ACKNOWLEDGEMENTS

We are indebted to Dr. C. Thessieu for directing our attention to the present subject. We also thank Professor A. Hasegawa for a valuable discussion. The present work is partially supported under the Grant in Aid for Scientific Research by the Ministry of Education, Japan.

*Electronic address: hyamada@gipac.shinshu-u.ac.jp

[1] Y. Ishikawa, K. Tajima, D. Bloch, and M. Roth, Solid State Commun. **19**, 525 (1976).
[2] D. Bloch, J. Voiron, V. Jaccarino, and J. H. Wernick, Phys. Lett. **51A**, 259 (1975).
[3] Y. Ishikawa, G. Shirane, J. Tarvin, and M. Kohgi, Phys. Rev. B **16**, 4956 (1977); Y. Ishikawa, Y. Noda, C. Fincher, and G. Shirane, *ibid.* **25**, 254 (1982).
[4] K. Motoya, H. Yasuoka, Y. Nakamura, and J. H. Wernick, Solid State Commun. **19**, 529 (1976).
[5] K. Makoshi and T. Moriya, J. Phys. Soc. Jpn. **44**, 80 (1978); K. Makoshi, *ibid.* **46**, 1767 (1979).
[6] O. Nakanishi, A. Yanase, and A. Hasegawa, J. Magn. Magn. Mater. **15-18**, 879 (1980).
[7] L. Taillefer, G. G. Lonzarich, and P. Strange, J. Magn. Magn. Mater. **54-57**, 957 (1986).
[8] C. Pfleiderer, G. J. McMullan, S. R. Julian, and G. G. Lonzarich, Phys. Rev. B **55**, 8330 (1997); C. Pfleiderer, Ph.D. thesis, The University of Cambridge, 1994.
[9] C. Thessieu, J. Flouquet, G. Lapertot, A. N. Stepanov, and D. Jaccard, Solid State Commun. **95**, 707 (1995); C. Thessieu, C. Pfleiderer, A. N. Stepanov, and J. Flouquet, J. Phys.: Condens. Matter **9**, 6677 (1997); C. Thessieu, Ph.D. thesis, University of Paris IV, 1995.
[10] E. P. Wohlfarth and P. Rhodes, Philos. Mag. **7**, 1817 (1962).
[11] M. Shimizu, J. Phys. (Paris) **43**, 155 (1982).
[12] T. Goto, K. Fukamichi, T. Sakakibara, and H. Komatsu, Solid State Commun. **72**, 945 (1989); T. Sakakibara, T. Goto, K. Yoshimura, and K. Fukamichi, J. Phys.: Condens. Matter **2**, 3381 (1990).
[13] K. Adachi, M. Matsui, and M. Kawai, J. Phys. Soc. Jpn. **46**, 1474 (1979).
[14] H. Hiraka and Y. Endo, J. Phys. Soc. Jpn. **65**, 3740 (1996).
[15] T. Goto, Y. Shindo, H. Takahashi, and S. Ogawa, Phys. Rev. B **56**, 14 019 (1997).
[16] H. Yamada, Phys. Rev. B **47**, 11 211 (1993).
[17] H. Yamada and K. Terao, J. Phys.: Condens. Matter **6**, 10 805 (1994).
[18] U. von Barth and L. Hedin, J. Phys. C **5**, 1629 (1972).
[19] V. L. Moruzzi, P. W. Marcus, K. Schwarz, and P. Mohn, Phys. Rev. B **34**, 1784 (1986).
[20] D. M. Edwards, J. Phys. F **12**, 1789 (1982).
[21] K. R. A. Ziebeck, P. J. Brown, J. G. Booth, and J. A. C. Bland, J. Phys. F **11**, L127 (1981).
[22] M. Uhl and J. Kübler, Phys. Rev. Lett. **77**, 334 (1996).
[23] M. Shimizu, Rep. Prog. Phys. **44**, 329 (1981).
[24] G. G. Lonzarich and L. Taillefer, J. Phys. C **18**, 4339 (1985).
[25] T. Moriya, *Spin Fluctuations in Itinerant Electron Magnetism* (Springer, Berlin, 1985).
[26] G. P. Zinoveva, L. P. Andereeva, and P. V. Geld, Phys. Status Solidi A **23**, 711 (1974).
[27] C. Thessieu, K. Kamishima, T. Goto, and G. J. Lapertot, J. Phys. Soc. Jpn. **67**, 3605 (1998).
[28] Y. Takahashi and T. Sakai, J. Phys.: Condens. Matter **7**, 6279 (1995).